

# Learning General Continuous Constraint from Demonstrations via Positive-Unlabeled Learning

Baiyu Peng Aude Billard  
École Polytechnique Fédérale de Lausanne (EPFL), Switzerland  
{baiyu.peng, aude.billard}@epfl.ch

**Abstract:** Planning for a wide range of real-world tasks necessitates to know and write all constraints. However, instances exist where these constraints are either unknown or challenging to specify accurately. A possible solution is to infer the unknown constraints from expert demonstration. The majority of prior works limit themselves to learning simple linear constraints, or require strong knowledge of the true constraint parameterization or environmental model. To mitigate these problems, this paper presents a positive-unlabeled (PU) learning approach to infer a continuous, arbitrary and possibly nonlinear, constraint from demonstration. From a PU learning view, We treat all data in demonstrations as positive (feasible) data, and learn a (sub)-optimal policy to generate high-reward-winning but potentially infeasible trajectories, which serve as unlabeled data containing both feasible and infeasible states. Under an assumption on data distribution, a feasible-infeasible classifier (i.e., constraint model) is learned from the two datasets through a postprocessing PU learning technique. The entire method employs an iterative framework alternating between updating the policy, which generates and selects higher-reward policies, and updating the constraint model. Additionally, a memory buffer is introduced to record and reuse samples from previous iterations to prevent forgetting. The effectiveness of the proposed method is validated in two Mujoco environments, successfully inferring continuous nonlinear constraints and outperforming a baseline method in terms of constraint accuracy and policy safety.

**Keywords:** Constraints inference, Inverse reinforcement learning, Learning from expert demonstrations

## 1 Introduction

Planning for many robotics and automation tasks also requires knowing constraints explicitly, which define what states or trajectories are allowed or must be avoided [1, 2]. Sometimes these constraints are initially unknown or hard to specify mathematically, especially when they are general, continuous, or inherent to an expert’s preference and experience. For example, human drivers may determine an implicit minimum distance from other cars based on traffic conditions, traffic rules, and even weather. To learn a driving policy matching human behaviors, an explicit constraint should be inferred somehow, e.g., from existing human demonstration sets.

A typical approach to recover the underlying constraint is through Inverse Constrained Reinforcement Learning (ICRL) [3, 4, 5]. It originates from Inverse Reinforcement Learning (IRL), a method to infer a reward function by observing the demonstrations of an expert [6]. In contrast to IRL, ICRL is developed exclusively to infer constraints instead of reward functions. A current

---

\*The authors are with the LASA, School of Engineering, EPFL (Swiss Federal Institute of Technology in Lausanne), Lausanne 1015 Vaud, Switzerland (e-mail: baiyu.peng@epfl.ch; aude.billard@epfl.ch). This work is funded by the ERC SAHR Grant.

major challenge of ICRL is that most methods are limited to recovering a linear constraint function or a nonlinear constraint with known parameterization. In this study, we will focus on this challenge and aim at learning a continuous (possibly nonlinear) constraint function on continuous state-action spaces. To see this, next we will review the existing constraint inferring methods, summarize their limitations, and explain the motivation of this work.

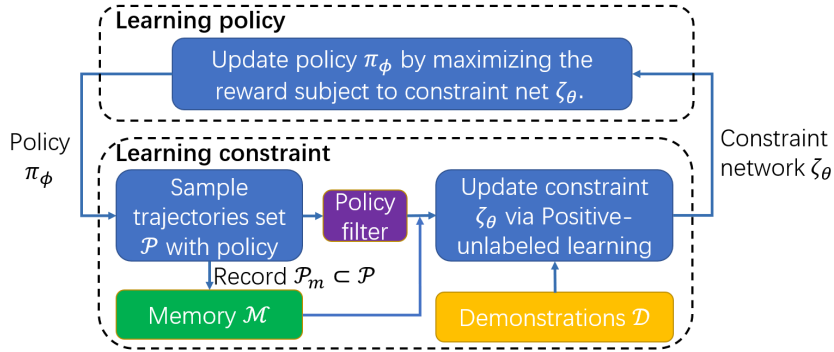


Figure 1: The framework of the proposed method. It alternates between two steps: learning policy and learning constraint. The first step updates the policy network by maximizing the reward subject to the already learned constraint. In second step, we utilize an PU learning approach to infer the unknown infeasible areas from both the demonstrated trajectories and the sampled potentially unsafe trajectories.

**Related Works:** Constraint inference through ICRL has drawn more and more attention since 2018. Chou et al. [7] first explores how to infer constraints given an environment model and a demonstration set. They assume that all possible trajectories that could earn higher rewards than the demonstration must be constrained in some way, or the expert could have passed those trajectories. In practice, they use hit-and-run sampling to obtain such higher reward trajectories and solve an integer program to recover the constrained states in a tabular environment. Scobee and Sastry [8] formalizes this idea by casting the problem in the maximum likelihood inference framework, which is also prevalent in the IRL domain. They introduce a Boltzmann policy model, where the likelihood of any feasible trajectory is assumed to be proportional to the exponential return of the trajectory, while the likelihood of any infeasible trajectory is 0. Then a greedy algorithm is proposed to add the smallest number of constraints that maximize the likelihood of the demonstrations. This framework has the advantage of being able to work with sub-optimal demonstrations. Alternatively, Vazquez-Chanlatte et al. [9] formulate a maximum a posterior probability inference problem to learn non-Markovian constraint, or task specifications. Further, Glazier et al. [10] and McPherson et al. [11] extend the maximum entropy framework from a deterministic setting into a stochastic setting, with soft or probabilistic constraints. In [10], they learn a residual reward (i.e., penalty) from demonstration using maximum entropy IRL. Assuming the penalty value follows a logistic distribution, the probability of constraint over features can be recovered. In [11], a causal entropy likelihood function is formulated and optimized via a modified version of soft Bellman backup, which is challenging to scale to continuous state-action spaces.

Unfortunately, all the methods mentioned above only apply to systems with discrete finite state spaces. To overcome this drawback, recent papers have made a few attempts to extend this to continuous cases. Stocking et al. [12] proposes an algorithm that learns a neural network policy via deep RL and generates high return trajectories with the policy network. Then the constraint is again added based on the maximum likelihood principle. However, like the previous methods, this method recovers constraints from a given constraint set. Besides, the method only works with a categorical action policy, not applied to a continuous policy. Recently, Malik et al. [3] proposes Maximum Entropy Constraint Learning (MECL) algorithm. It not only approximates the policy with a network but also learns a constraint network, a continuous function that can represent more general constraints. This constraint network is optimized by making a gradient ascent

on the maximum likelihood objective function. Although theoretically the method can arbitrary constraint on continuous state spaces and constraints, in practice it was only applied to recover plane constraints, e.g.  $x \geq -3$  [3], and, as we show later in the paper, performs relatively poorly at learning more complex constraints. This is partly due to an unrecognized problem of constraint forgetting that we discuss later in section 2.4. In parallel, in Inverse Optimal Control community, another line of research based on KKT optimality condition has been developed to learn general continuous constraints [13, 14], but these methods require a closed-form model and its derivative, which are not always available in reality.

In summary, despite impressive advances to solve ICRL, it still remains to be shown that ICRL can be used to learn continuous nonlinear constraint functions from a small sample of demonstrations in a model-free manner.

To overcome the aforementioned challenge, we propose a novel positive-unlabeled approach to learn an arbitrary and continuous constraint function in continuous state-action spaces. Our method is inspired by a machine learning subarea Positive-Unlabeled (PU) learning [15], and to best of our knowledge, this work is the first to handle the constraint inference problem from a PU learning perspective. We treat all data in demonstrations as positive (feasible) dataset, and learn a policy to generate many potentially unsafe trajectories, which contains unlabeled states that could be feasible or infeasible. Then a postprocessing PU learning technique is applied to identify the truly infeasible states from the two dataset. It makes an assumption on data distribution, and synthesises the feasible-infeasible classifier (i.e., constraint model) from a feasible-unlabeled classifier with a moved classification threshold.

To generate potentially unsafe trajectories, we also maintain a constrained RL policy that always maximizes the reward function subject to the current constraint function. If the policy achieves a higher reward than the demonstration assumed to be (sub-)optimal, we believe it implies that the policy must have explored certain unknown unsafe states to win such a high reward [7].

Our constraint learning paradigm is phrased as an iterative framework, see Fig. 1. At each iteration, we first train a policy maximizing the reward subject to the constraints. Then, a set of higher-reward trajectories are generated by sampling from the policy, which are further used along with the demonstrations to infer constraints via PU learning technique. In the next iteration, the new policy is updated with respect to the new constraints. To prevent forgetting the previously learned constraints, a memory mechanism is introduced, where some most representative infeasible states are recorded and used for training in the following interactions.

## 2 Method

### 2.1 Preliminaries and Problem Statements

For a Markov decision process (MDP) [16, 17], states and actions are denoted by  $s \in \mathcal{S}$  and  $a \in \mathcal{A}$ .  $\gamma$  denotes the discount factor, and the real-valued reward is denoted by  $r(s, a)$ . Note that in ICRL, reward is usually assumed to be given [3, 7]. A trajectory  $\tau = \{s_1, a_1, \dots, s_T, a_T\}$  contains a sequence of state-action pairs in one episode. For the trajectory  $\tau$ , the total discounted reward (return) is defined as  $r(\tau) = \sum_{t=1}^T \gamma^t r(s_t, a_t)$ . A policy, the mapping between states and actions, is denoted by  $\pi(a|s)$ . Note that different from [13, 14], we do not make the assumption of possessing a closed-form model or its derivatives of the transition dynamics. We only assume a simulator is available that can simulate the dynamics and return the next state and reward, but no information about the true constraint is included.

The true constraint set  $\mathcal{C}^*$  consists of all the actually infeasible states  $\mathcal{C}^* = \{s \in \mathcal{S} | s \text{ is actually infeasible}\}$ . Note that for simplicity of explanation, we only consider a state constraint, but it can be easily extended to state-action constraints by augmenting the state with the action to form an augmented state. We aim to recover the true constraint set from the demonstration. Suppose we have collected a set of demonstrated trajectories  $\mathcal{D} = \{\tau^i\}_{i=1}^{M_d}$  generated from an expert  $\pi^*$  navigating in the true environment. We assume that the expert  $\pi^*$  maximizes the

return  $J(\pi) = \mathbb{E}_{\tau \sim \pi} \{r(\tau)\}$  while never visiting the truly infeasible states. To represent and learn an arbitrary constraint set in continuous state space, we define a continuous constraint function  $\zeta_\theta(s) \in (0, 1)$  and its induced constraint set  $\mathcal{C}_\theta = \{s \in \mathcal{S} | \zeta_\theta(s) \leq d\}$ , where  $\theta$  is the function parameter and  $d$  is a manually specified threshold. The constraint function  $\zeta_\theta$  can be regarded as the probability that a state is feasible, while  $d$  serves as the decision threshold. We further define a binary constraint indicator function  $c_\theta(s)$  to represent the feasibility of a state.

$$c_\theta(s) = \begin{cases} 0 & \text{if } \zeta_\theta(s) > d \text{ (feasible)} \\ 1 & \text{if } \zeta_\theta(s) \leq d \text{ (infeasible)} \end{cases} \quad (1)$$

## 2.2 Constraint Inference as Positive-Unlabeled Learning

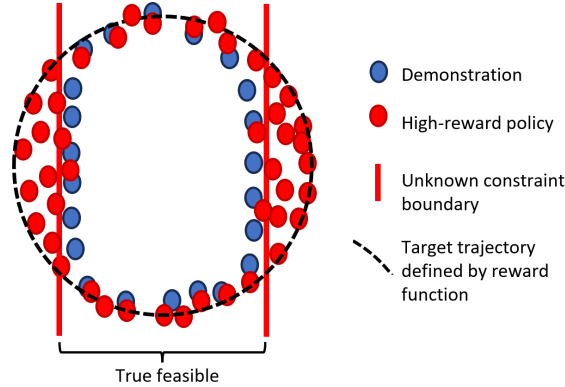


Figure 2: The illustration of constraint inference from the PU learning perspective and the example of SCAR assumption. The red dots denote states from the demonstration, the blue dots denote states from the high-reward trajectory, the red lines denote the unknown constraint boundary and black circle denote the target trajectory given by the reward function.

As discussed before, we infer the underlying constraint by contrasting the demonstration with a high-reward-winning policy. In each iteration, we first sample a set of high-reward trajectories  $\mathcal{P} = \{\tau_p^i\}_{i=1}^{M_p}$  by performing current policy  $\pi_\phi$  (discussed later in 2.3). Each sampled trajectory consists of sequential state-action pairs  $\tau_p = \{s_j, a_j\}_{j=1}^{N_i}$ . We speculate that the higher-reward trajectory wins high reward by violating some unknown constraints. However, it remains unclear which specific state(s) within the trajectory has violated the constraint. In another word, trajectory  $\tau_p$  consist of both feasible states and infeasible states but both remains unlabeled. In contrast, it is certain that all states on the demonstrated trajectories are labeled as feasible. Our goal is to classify each single state as feasible or infeasible by learning from a batch of fully labeled feasible samples and another batch of unlabeled samples.

This insight inspires us to formulate constraint inference as a positive-unlabeled learning problem, which learns from only a positive dataset and an unlabeled dataset containing both positive and negative samples [15]. Within our framework, feasible states are designated as positive samples. Consequently, the demonstrations serve as positive samples, while the policy offers unlabeled samples with unknown feasibility. Any datapoint can be represented as a set of triplets  $(s, c, l)$  with  $s$  the state,  $c$  the class (1 for feasible), and  $l$  a binary variable representing whether the tuple is labeled. If a sample is labeled (i.e.,  $l = 1$ ), it must originate from the demonstration and is sure to be feasible, i.e.,  $Pr(c = 1 | l = 1) = 1$ . A key quantity from PU learning is the label frequency  $f$ , which is defined as the proportion of positive samples that are labeled within the entire dataset:

$$f = Pr(l = 1 | c = 1) = \frac{Pr(l = 1)}{Pr(c = 1)} \quad (2)$$

In the constraint learning context, the label frequency  $f$  implies the sparsity of the truly feasible states in the state space. A high value  $f$  suggests that the majority of truly feasible states are

distributed on the demonstrated trajectories and thus labeled, while only a few amount of feasible states are on the higher-reward trajectory and thus unlabeled. Subsequently, we introduce an assumption regarding the labeling mechanism [15]:

**Assumption 1** (*Selected Completely At Random (SCAR)*) *Labeled samples are selected completely at random, independent of states. For any truly feasible state, its probability of being demonstrated and labeled is constant and equal to the label frequency:*

$$Pr(l = 1|s, c = 1) = Pr(l = 1|c = 1) = f \quad (3)$$

Intuitively, the SCAR assumption requires that among all the truly feasible states, those visited more frequently by the expert should also be more frequently visited by the policy. In other words, apart from truly infeasible regions, the expert and the policy should exhibit similar behaviors and have similar state distribution elsewhere. An example for SCAR assumption and PU learning is given in Fig. 2. Consider a planar task called point-circle, a point robot is rewarded for running in a wide circle, but is constrained to stay within a narrow region smaller than the radius of the target circle. The high-reward policy and demonstration have similar distribution inside the truly feasible area, i.e., the area between the two boundary.

Subsequently we introduce a postprocessing approach [18] for uncovering the unknown infeasible regions due to its 1) inherent simplicity and 2) compatibility with various models, including neural networks. Given the SCAR assumption, the probability of an sample being labeled is directly proportional to the probability of that sample being positive:

$$\begin{aligned} Pr(l = 1|s) &= Pr(c = 1, l = 1|s) \\ &= Pr(c = 1|s)Pr(l = 1|c = 1, s) \\ &= Pr(c = 1|s)Pr(l = 1|c = 1) \\ &= fPr(c = 1|s) \end{aligned} \quad (4)$$

which leads to

$$Pr(c = 1|s) = \frac{1}{f}Pr(l = 1|s) \quad (5)$$

Consequently, it is evident that a labeled-unlabeled classifier, trained to predict  $Pr(l|s)$  by treating unlabeled data as negative and labeled data as positive, can be directly employed to forecast the class probabilities  $Pr(c = 1|s)$  and predict the class [18]. Alternatively, noticing that  $Pr(c = 1|s) > 0.5$  is equivalent to  $Pr(l = 1|s) > 0.5f$ , the labeled-unlabeled classifier can be repurposed as a feasible-infeasible classifier by directly adjusting the decision threshold from  $d = 0.5$  to  $d = 0.5f$ .

Based on the above derivation, we initiate the process by training a labeled-unlabeled classifier  $\zeta_\theta(s)$ , which outputs the labeled probability  $Pr(l = 1|s)$ . It is trained through gradient descent utilizing the binary cross entropy (BCE) loss as in (6). Within the training set, states from  $\mathcal{D}$  serve as positive samples, while those from  $\mathcal{P}$  are treated as negative samples.

$$\mathcal{L}(\theta) = -\frac{1}{N} \sum_{s_i \sim \mathcal{D}} \log \zeta_\theta(s_i) - \frac{1}{M} \sum_{s_j \sim \mathcal{P}} \log(1 - \zeta_\theta(s_j)), \quad (6)$$

Once trained, this classifier can be directly employed as a feasible-infeasible classifier by setting the decision threshold to  $d = 0.5f$  as in (7).

$$c_\theta(s) = \begin{cases} 1 & \text{if } \zeta_\theta(s) > 0.5f \text{ (feasible)} \\ 0 & \text{if } \zeta_\theta(s) \leq 0.5f \text{ (infeasible)} \end{cases} \quad (7)$$

The subsequent work involves determining the label frequency  $f$ . Estimating  $f$  is a central concern in PU learning, with diverse methods such as partial matching and kernel embedding being proposed [15]. In this work, we suggest two approaches. A conventional and straightforward approach [19] uses the insight that  $Pr(l = 1|s) = fPr(c = 1|s)$ , which is equal to the label frequency  $f$  when the

true class probability is  $Pr(c = 1|s) = 1$ . Suppose there will be state for which  $Pr(c = 1|s) \approx 1$ , the label frequency can be hence estimated as  $f = \max_{s \in \mathcal{D}} \zeta_\theta(s)$ . Alternatively, recall that  $f$  indicates the density of infeasible states in the state space, it can be reviewed as a hyper-parameter representing the user’s belief over the constraint density. A higher value of  $f$  suggests a denser distribution of infeasible states. In our following experiments, we adopt the latter perspective and set  $f = 0.4$ .

Lastly, to mitigate over-fitting, we incorporate the following regularization term into the loss function (6):

$$\mathcal{L}_r(\theta) = -w_r \frac{1}{N_r} \sum_{s_i \sim \mathcal{S}} \zeta_\theta(s_i) \quad (8)$$

where  $w_r$  is the a fixed regularization weight. The state  $s_i$  is uniformly sampled from the whole state space.

### 2.3 Policy Learning via Constrained RL

In order to generate high-reward trajectories while satisfying the already learned constraints, an RL policy network is established and maintained during the learning process. Akin to some recent works [5, 20], this paper adopts a popular and relatively simple algorithm PPO-penalty [21] for constrained policy optimization. As shown in (9), it reshapes the original reward by turning the constraint as a penalty term into the original reward function to avoid the infeasible states, where  $w_p$  is a fixed penalty weight and  $c(s)$  is a constraint indicator defined in (1). Hence, a constrained optimal policy can be straightforwardly learned by optimizing the reshaped reward  $r'(s, a)$  with the standard deep RL algorithm PPO [21].

$$r'(s, a) = r(s, a) - w_p c_\theta(s) \quad (9)$$

It is worth noting that some ICRL researches employ PPO-Lagrangian [3] instead of PPO-penalty. Although PPO-Lagrangian offers the advantage of automatically adjusting the penalty weight, it is also known to introduce high instability, resulting in significant oscillations in the policy’s performance during training and making convergence difficult [22]. When applying PPO-Lagrangian to ICRL where the constraint function itself changes over iterations, the issue of instability becomes even more detrimental: the oscillation in learning the policy will propagate to learning the constraint function, leading to further instability in learning the policy. Recent works have also observed this problem and therefore chosen the penalty method instead of the Lagrangian method [5, 20].

The learning is in an iterative framework alternating between learning constraint and learning policy. Normally, it can be very time-consuming to train the policy until convergence in every iteration. Similar to related works [3, 4], we only perform limited timesteps in policy updating to save time. However, in practice, we notice that this mechanism occasionally leads to catastrophic results. Suppose that in some iteration it accidentally learns a very poor policy. Recall that we are inferring the constraint through the difference between demonstration and policy, and a poor policy obviously does not contain any meaningful information about true constraint. Therefore, the poor policy will in turn lead to a poor (usually redundant) constraint, and to an even poorer policy. Finally, the algorithm collapses. To mitigate this drawback, we propose to introduce a policy filter (see Fig. 1) that only lets pass the sampled trajectories with relatively high reward than demonstration, which are believed to violate the unknown constraint to be inferred. Concretely, the trajectory  $\tau_i$  can pass the filter if its return satisfies

$$r(\tau_i) \geq r_{\mathcal{D}} - \alpha \sigma_{\mathcal{D}} \quad (10)$$

where  $r_{\mathcal{D}}$  and  $\sigma_{\mathcal{D}}$  are respectively the mean and standard deviation of return among all demonstrated trajectories,  $\alpha$  is a hyperparameter and is always selected as 1 in this work.

### 2.4 Constraint Memory Replay

When learning complex constraints with approximation functions in an iterative manner, a problem of "constraint forgetting", which has not been well recognized and studied in similar papers [3, 12],

will emerge. The forgetting problem is demonstrated in Fig. 3: suppose there are two unknown rectangular constrained areas shown in red. In the first iteration, by contrasting policy with demonstration, the left infeasible area is uncovered. But in the second iteration, when the policy shifts and leaves the left infeasible area, there is no more data in that area. If we update the constraint model with data only from iteration 2, the left area may become feasible again due to some approximation error. This problem will become especially apparent in iteration 3: when the policy and demonstration almost overlap, updating the constraint network with data from iteration 3 will have a very random influence over the model. The noise in policy learning and function approximation may well make the model forget the already learned constrained areas.

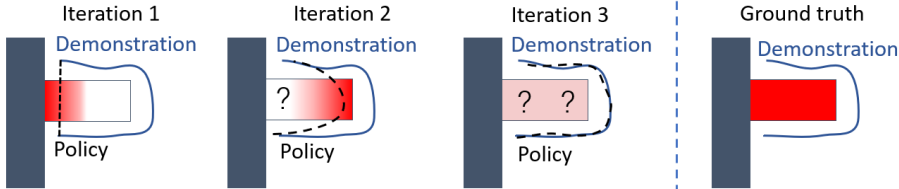


Figure 3: Illustration of "forgetting" problem, where the constrained areas already learned in previous iterations may be forgotten later. The trajectories of the demonstrations and the policy are shown in blue and black, respectively. The red rectangle represents the constrained areas to be inferred.

We call the above phenomenon a "forgetting" problem. Note that this is not a problem if we are recovering finite infeasible states from a discrete grid world, where the infeasible states are added to the constraint set in a one-by-one manner, and the constraint once learned will be kept forever [7, 8]. But when learning constraints with a continuous approximation function, the constrained area learned in previous iterations may be forgotten due to noise in function approximation and policy. One possible remedy is to enhance the exploration and try multiple strategies at the same time to cover more state spaces. But as discussed in [12], a usual Gaussian policy is not enough and a categorical discrete action policy is necessary, which does not apply to continuous action space.

To mitigate this problem, we propose the constraint memory replay mechanism (CMR). From Fig. 3, we speculate the sampled trajectories at each iteration contain information about a certain constrained area. Ideally, if we record some of the trajectories  $\mathcal{P}_m \subset \mathcal{P}$  in each iteration and keep using them for training in the following iterations, the constraint will not be forgotten. In practice, instead of recording the whole trajectories, we find that it is better to record only a batch of states that are most likely to be infeasible, because 1) it is beneficial to avoid overfitting (i.e., learning an overly large constrained area); 2) it saves the memory and computation resources. Specifically, in each iteration, we rank from low to high all the infeasible states from sampled trajectories (i.e.,  $\{s \in \mathcal{P} | c_\theta(s) = 0\}$ ) by their constraint value  $\zeta(s)$ , and save only the top  $1/N_m$  portion of states into a memory buffer  $\mathcal{M}$  ( $N_m$  is a parameter). These recorded states have the lowest  $\zeta(s)$  values, and are regarded as representatives of the constraint learned in that iteration.

Fig. 1 gives a sketch of the whole iterative structure with the memory replay mechanism. The pseudo-code for the algorithm is given in Algorithm 1.

### 3 Experiment

#### 3.1 Experiment Setup

**Environments:** Two environments, namely point-circle, point-obstacle and ant-wal, have been considered to examine the performance of the proposed method (see Fig. 4). In both environments, the agent is a point robot moving in 2-D plane. In the point-circle, the aim is to encourage the agent to follow a circle; however, the agent is constrained to stay within a narrow region smaller than the defined circle. In the point-obstacle, the agent is initialized from somewhere at the bottom of the environment and is rewarded for reaching a target above while avoiding a rectangular obstacle in the

---

**Algorithm 1** Learning continuous constraint function from demonstration

---

**input:** Demonstration set  $\mathcal{D}$ , randomly initialized constraint network  $\zeta_\theta$ , randomly initialized policy network  $\pi_\phi$ , empty memory buffer  $\mathcal{M} = \emptyset$

**repeat**

**% Learning policy step**

  Updating the policy  $\pi_\phi$  with the reward (10) penalized with current constraint model  $\zeta_\theta$

**% Learning constraint step**

  Sample a set of trajectories  $\mathcal{P}$  with the current policy  $\pi_\phi$

  Filter  $\mathcal{P}$  and remove poor trajectories not satisfying (10)

  Update the constraint network  $\zeta_\theta$  with the demonstration, filtered trajectories and memory:

$$\mathcal{L}(\theta) = -\frac{1}{N} \sum_{s_i \sim \mathcal{D}} \log \zeta_\theta(s_i) - \frac{1}{M} \sum_{s_j \sim \mathcal{P} \cup \mathcal{M}} \log(1 - \zeta_\theta(s_j)) - w_r \frac{1}{N_r} \sum_{s_k \sim \mathcal{S}} \zeta_\theta(s_k)$$

  Save the a batch of representative states  $\{s_i\} \in \mathcal{P}$  into the memory buffer  $\mathcal{M} \leftarrow \mathcal{M} \cup \{s_i\}$  based on the principle in 2.4

**until** meet some stop criterion

---

middle. Note that the constraints in the two environments are more complex and nonlinear compared with those considered in the related papers [3, 4], which only learns a plain constraint like  $x \geq -3$ . The expert demonstration set consists of 20 safe trajectories generated by an entropy-regularized RL agent, trained assuming full knowledge of the true constraint.

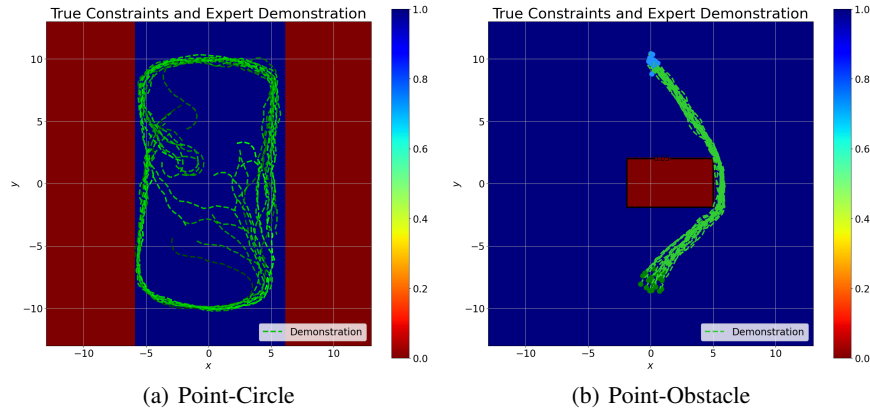


Figure 4: True constraints and expert demonstration. The green dotted lines are 20 expert trajectories. The x-axis and y-axis are exactly the coordinates of the point robot. The colormap visualizes true constraint function  $\zeta^*(x, y)$ , where the red area is the truly constrained area to be inferred, while the blue area is feasible.

**Metrics:** Several different metrics have been employed in the literature to quantify the correctness of the learned constraint. Recent methods working with neural network constraints often consider the policy’s performance, such as constraint violation or reward, when trained with the NN constraint and tested in the true constrained environment [3, 4, 20]. However, we argue that solely comparing the performance of the learned policy may lead to misleading results, as the performance is significantly influenced by the performance of specific constrained RL algorithm employed. A detailed discussion of metric selection, accompanied by an example of misleading results of a prior paper [3], is provided in Appendix 5.2. In this study, we present the evaluation of policy learning performance by utilizing two metrics: 1) the IoU (the intersection over union) index to measure the correctness of the learned constraints; we uniformly sample points in the state space, and compute IoU as (Number of points which are both predicted to be infeasible and truly infeasible) divided by (Number of points either predicted to be infeasible or truly infeasible); 2) the per-step true constraint violation rate of the learned policy. Additionally, we provide visualizations of the constraint network output to offer an intuitive understanding of the learning outcomes.

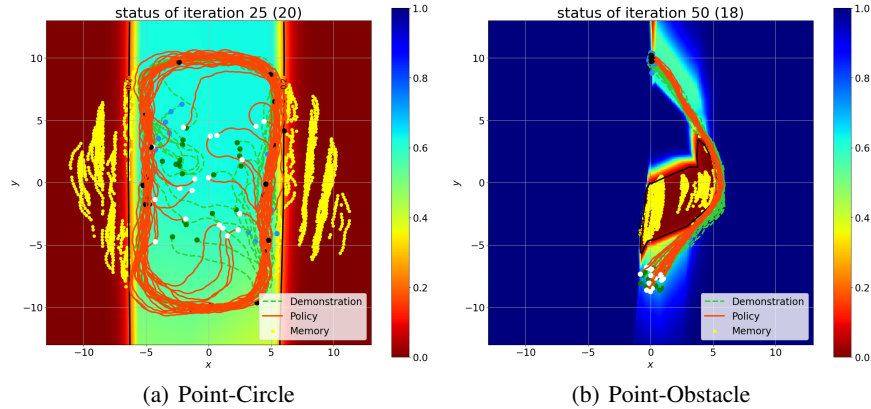


Figure 5: Constraints learned with the proposed method. The trajectories of the demonstrations and the policy are shown in green and red, respectively. The yellow points correspond to data stored in the memory buffer. The learned constrained areas are represented by the red regions, while the (light) blue regions indicate feasibility.

### 3.2 Results

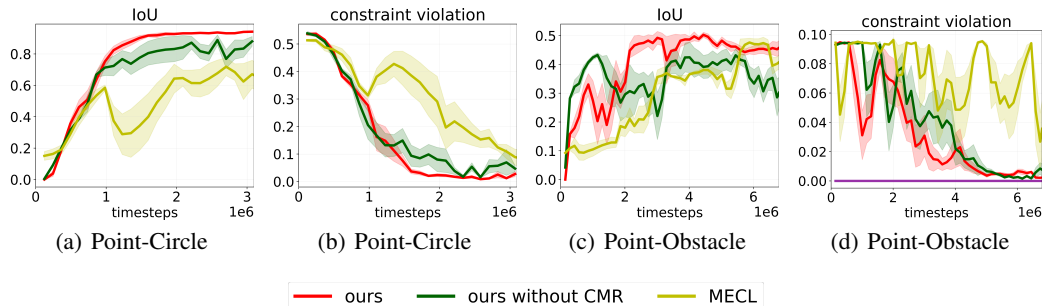


Figure 6: The IoU index (higher is better) and constraint violation rate (lower is better) of learned constraint function. The left two figures are for environment point-circle while the right two are for environment point-obstacle. The x-axis corresponds to the number of timesteps the agent takes in the environment. Our method outperforms the baseline method in both environments.

We compare the constraint learning performance of the three methods: 1) the propose method, 2) the proposed method without CMR (constraint memory replay), and 3) a popular ICRL method MECL [3]. The IoU index and constraint violation rate in the first two environments are presented in Fig. 6. All the results are the average of 5 independent runs, and the shaded area represents the variance. The 5 runs use the same demonstrations and hyper-parameters, but differ in the initialization parameters for the policy and constraint networks.

**Overall Performance:** The proposed methods exhibit superior performance compared to the baseline across both environments and metrics. This distinction is particularly large in Point-Obstacle, characterized by a nonlinear and non-convex constraint. Besides, the baseline suffers from strong performance oscillation, while our method achieves a more stable learning process. This is partly caused by the forgetting problem we discussed in 2.4, i.e., it keeps learning and forgetting the constraint during training.

**Ablation Study of Constraint Memory Replay:** Comparing the performance of our method and our method without CMR, we conclude the CMR technique enhances the precision of learned constraints. This improvement is particularly evident in the Point-Obstacle environment in terms of IoU, where the method without CMR undergoes a decline in performance (i.e., constraint forgetting)

around  $2e6$  and  $6e6$  timesteps. However, the performance gap in terms of constraint violation is relatively smaller, primarily because constrained states in proximity to the boundary are frequently visited and less prone to forgetting, thus having less influence on the constraint violation. This observation also aligns with our illustrative insights provided in Figure 3.

**Visualization:** To provide readers with a better understanding, we include visualizations of the learned constraint when our method reaches convergence. Comparing the learned constraints in Fig. 5 with the true constraints displayed in Fig. 4 confirms the effectiveness of our method in acquiring a model of both linear and nonlinear constraints. While the learned constraint area is partially incorrect, it effectively captures the essence of the true constraint and proves sufficient for training a safe policy. Additionally, we observe that the memorized data points are distributed within the infeasible areas, thereby aiding in preventing the constraint network from forgetting previously learned constraints. These visualizations provide a clear demonstration of the advantages offered by the memory introduced in 2.4.

## 4 Conclusions

This paper proposed an positive-unlabeled constraint Learning method to infer from demonstration an arbitrary continuous constraint on continuous state spaces. The proposed method treats the demonstration as the positive data and the higher-reward-winning policy as the unlabeled data, and thus trains a feasibility classifier from the two datasets via a postprocessing PU learning technique. In addition, a memory mechanism was introduced to prevent forgetting. The benefits of the proposed method were demonstrated in two robotics tasks. It managed to recover the continuous nonlinear constraints and outperforms a baseline method in terms of accuracy and constraint violation. In the future, we will apply the proposed method to more high-dimensional environments with more complex constraints.

## References

- [1] J. Garcia and F. Fernández. A comprehensive survey on safe reinforcement learning. *Journal of Machine Learning Research*, 16(1):1437–1480, 2015.
- [2] R. Noothigattu, D. Bouneffouf, N. Mattei, R. Chandra, P. Madan, K. R. Varshney, M. Campbell, M. Singh, and F. Rossi. Teaching ai agents ethical values using reinforcement learning and policy orchestration. *IBM Journal of Research and Development*, 63(4/5):2–1, 2019.
- [3] S. Malik, U. Anwar, A. Aghasi, and A. Ahmed. Inverse constrained reinforcement learning. In *International Conference on Machine Learning*, pages 7390–7399. PMLR, 2021.
- [4] G. Liu, Y. Luo, A. Gaurav, K. Rezaee, and P. Poupart. Benchmarking constraint inference in inverse reinforcement learning. *International Conference on Learning Representations*, 2023.
- [5] D. Papadimitriou, U. Anwar, and D. S. Brown. Bayesian methods for constraint inference in reinforcement learning. *Transactions on Machine Learning Research*, 2022.
- [6] S. Arora and P. Doshi. A survey of inverse reinforcement learning: Challenges, methods and progress. *Artificial Intelligence*, 297:103500, 2021.
- [7] G. Chou, D. Berenson, and N. Ozay. Learning constraints from demonstrations. In *Algorithmic Foundations of Robotics XIII: Proceedings of the 13th Workshop on the Algorithmic Foundations of Robotics 13*, pages 228–245. Springer, 2020.
- [8] D. R. Scobee and S. S. Sastry. Maximum likelihood constraint inference for inverse reinforcement learning. In *International Conference on Learning Representations*, 2020.
- [9] M. Vazquez-Chanlatte, S. Jha, A. Tiwari, M. K. Ho, and S. Seshia. Learning task specifications from demonstrations. *Advances in neural information processing systems*, 31, 2018.
- [10] A. Glazier, A. Loreggia, N. Mattei, T. Rahgooy, F. Rossi, and B. Venable. Learning behavioral soft constraints from demonstrations. *arXiv preprint arXiv:2202.10407*, 2022.
- [11] D. L. McPherson, K. C. Stocking, and S. S. Sastry. Maximum likelihood constraint inference from stochastic demonstrations. In *2021 IEEE Conference on Control Technology and Applications (CCTA)*, pages 1208–1213. IEEE, 2021.
- [12] K. C. Stocking, D. L. McPherson, R. P. Matthew, and C. J. Tomlin. Maximum likelihood constraint inference on continuous state spaces. In *2022 International Conference on Robotics and Automation (ICRA)*, pages 8598–8604. IEEE, 2022.
- [13] G. Chou, N. Ozay, and D. Berenson. Learning constraints from locally-optimal demonstrations under cost function uncertainty. *IEEE Robotics and Automation Letters*, 5(2):3682–3690, 2020.
- [14] G. Chou, H. Wang, and D. Berenson. Gaussian process constraint learning for scalable chance-constrained motion planning from demonstrations. *IEEE Robotics and Automation Letters*, 7(2):3827–3834, 2022.
- [15] J. Bekker and J. Davis. Learning from positive and unlabeled data: A survey. *Machine Learning*, 109:719–760, 2020.
- [16] R. S. Sutton and A. G. Barto. *Reinforcement learning: An introduction*. MIT press, 2018.
- [17] E. Altman. *Constrained Markov decision processes*, volume 7. CRC press, 1999.
- [18] C. Elkan and K. Noto. Learning classifiers from only positive and unlabeled data. In *Proceedings of the 14th ACM SIGKDD international conference on Knowledge discovery and data mining*, pages 213–220, 2008.

- [19] T. Liu and D. Tao. Classification with noisy labels by importance reweighting. *IEEE Transactions on pattern analysis and machine intelligence*, 38(3):447–461, 2015.
- [20] A. Gaurav, K. Rezaee, G. Liu, and P. Poupart. Learning soft constraints from constrained expert demonstrations. In *International Conference on Learning Representations*, 2023.
- [21] J. Schulman, F. Wolski, P. Dhariwal, A. Radford, and O. Klimov. Proximal policy optimization algorithms. *arXiv preprint arXiv:1707.06347*, 2017.
- [22] A. Stooke, J. Achiam, and P. Abbeel. Responsive safety in reinforcement learning by pid lagrangian methods. In *International Conference on Machine Learning*, pages 9133–9143. PMLR, 2020.

## 5 Appendix

### 5.1 Detailed Experiment Setup

As shown in Fig. 4, two environments, named point-circle and point-obstacle, have been developed in MuJoCo for assessing the performance of the proposed framework. In both environments, the state space is three-dimensional, i.e., the state vector is  $s := [x, y, \psi]^\top$ , where  $x, y$  are the positional coordinates of the point robot in the plane, and  $\psi$  is the heading angle. Moreover, the action vector in both environments is the two-dimensional vector  $a := [\|v\|_2, \omega]^\top$ , where  $\|v\|_2$  is the magnitude of the linear velocity, and  $\omega$  is the angular velocity. Both of the actions are limited to the  $[-0.25, 0.25]$  range.

The agent in the point-circle environment is a point robot that is rewarded to follow a circle with a radius of  $d = 10$  in a clockwise trend. However, there exist two walls at  $x = \pm 6$ , which prevents the full circular motion encouraged by the reward and forces the agent to remain within  $-6 \leq x \leq 6$ . The corresponding reward function is formulated in (11), where  $dx = \|v\|_2 \cos(\psi)$  and  $dy = \|v\|_2 \sin(\psi)$ .

$$r(s) = \frac{ydx - xdy}{1 + \left| \| [x, y]^\top \|_2 - d \right|} \cdot \frac{1}{\| [x, y]^\top \|_2} \quad (11)$$

In the point-obstacle environment, the same point robot is tasked to reach a target  $G$  at  $[G_x, G_y]^\top = [0, 10]^\top$  starting from a random position around  $[x, y]^\top = [0, -8]^\top$  which is below the rectangular obstacle that is situated in the middle ( $-2 \leq x \leq 5$  and  $-2 \leq y \leq 2$ ). In addition, it is assumed that there is a known wall to the left of this obstacle such that the  $x \leq -2$  region is inaccessible for the agent, meaning that the robot can only go around the obstacle from the right. The associated reward function is defined in (12), where  $f = 20$  is a normalization factor. A value of 0.1 is added to this reward in case the agent reaches the vicinity of the target (distance smaller than 0.3).

$$r(s) = -\frac{\sqrt{(x - G_x)^2 + (y - G_y)^2}}{f} \quad (12)$$

A list of important hyperparameters for both environments employed in both MECL and our frameworks is given in 1. The hidden activation functions in both constraint and policy neural networks are Leaky ReLU. Moreover, the output activation function for the constraint network is the sigmoid function, whereas that of the policy network is tanh.

### 5.2 Discussion on Metrics for Performance Assessment

Several metrics have been proposed in the literature to measure the constraint learning performance, i.e., how good the learned constraints are with respect to the true constraints. The metrics can be divided into two classes. The first class is concerned with the direct evaluation of the learned constraint set by comparing it with the true constraint set [7, 8]. These metrics are mostly applied in grid world scenarios, where the correspondence between learned and true constraints can be checked state by state, and the accuracy or recall rate can be computed accordingly. Despite examining the learned constraints directly, these types of metrics treat all infeasible states equally, but generally speaking the states near the boundary of the constraint should be of greater importance.

The second set of metrics, more used for the NN-based methods, is designed by calculating the reward or the rate of constraint violation of the learned policy in a testing environment [3, 4]. As such, if the constraint violation rate is low and the reward is high, they believe the constraint is well-learned. Although these metrics can be effortlessly applied in continuous state spaces, they are significantly affected by how the policy is learned since they do not directly take into account the learned constraints. More specifically, even if two policies learn exactly the same constraints, they can still possess different performances due to some minor differences or noises in policy learning.

The reason behind the above statement can be better motivated by a case study of a misleading result reported in the previous paper [3]. We re-run their [original implementation](#) in the HalfCheetah

Table 1: List of hyperparameters. For the neural network architectures, the number of hidden units in each layer is mentioned.

Hyperparameter	Point-Circle (Ours)	Point-Circle (MECL)	Point-Obstacle (Ours)	Point-Obstacle (MECL)
Policy, $\pi_\phi$				
Policy Network	16, 16	16, 16	16, 16	16, 16
Value Network	16, 16	16, 16	16, 16	16, 16
Learning Rate	$3 \times 10^{-4}$	$3 \times 10^{-4}$	$3 \times 10^{-4}$	$3 \times 10^{-4}$
Entropy Coefficient	0.01	0.01	0.01	0.01
Penalty Weight, $w_p$	0.5	0.5	0.7	0.9
Forward Iterations	5	5	6	6
Forward Timesteps	20,000	20,000	20,000	20,000
Constraint, $\zeta_\theta$				
Network	4	4, 4	16, 16	16, 16
Learning Rate	0.03	0.005	0.03	0.03
Backward Iterations	20	20	20	20
Regularization Weight, $w_r$	0.05	0.1	0.25	0.1
Decision Threshold, $d$	0.2	-	0.05	-
Memory Fraction, $N_m$	2	-	2	-
Miscellaneous				
Iterations	25	25	50	50
Expert Trajectories	20	20	20	20
Expert Trajectory Length	150	150	175	175

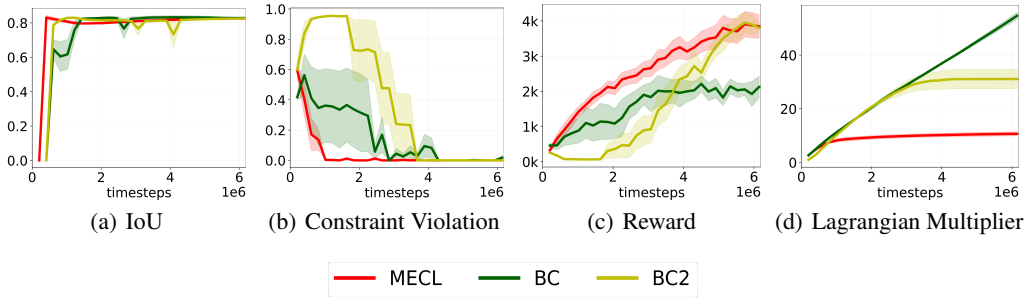


Figure 7: The intersection over union (IoU) metric (higher is better), constraint violation rate (lower is better), reward (higher is better), and the Lagrangian multiplier ( $\lambda$ ) for the MECL method and binary cross-entropy (BC) method discussed in [3] alongside BC modified by us (BC2). The x-axis corresponds to the number of timesteps the agent takes in the environment. These figures are obtained using the original implementation of [3] in the HalfCheetah environment.

environment, which consists of an 18-dimensional state space and a 6-dimensional action space. The reward in this environment is proportional to the distance the HalfCheetah robot covers at each step. Fig. 7 presents IoU, constraint violation, reward, and the Lagrangian multiplier during learning. Note that the original paper evaluated only the reward and constraint violation, based on which they concluded that MECL is superior in constraint learning compared to the binary cross-entropy (BC) method. We argue that this conclusion is imprecise. As shown in Fig. 7(a), the IoU suggests the same correctness learned by two methods. We dug into this issue and determined that it is actually caused by inappropriate settings in constrained RL.

The two methods both adopt PPO-Lagrangian for constrained RL. However, when the same state  $s$  is visited by the policy and expert demonstration, the MECL loss makes  $\zeta(s) = 0$  while BC makes  $\zeta(s) = 0.5$ . Thus, BC will accumulate cost bigger than zero all the time. Since [3] uses the budget of  $\alpha = 0$  for both methods, for BC, the Lagrange multiplier ( $\lambda$ ) keeps increasing (see Fig. 7(d)), but for MECL it stops at a reasonable value. With a too large  $\lambda$ , BC will win less reward than the MECL even though they actually learn a constraint network nearly equally good in terms of IoU.

To further verify this, we repeat the same experiment for BC but with a feasibility decision threshold of  $d = 0.2$ , i.e., only  $\zeta(s) < 0.2$  will be regarded as infeasible and accumulate cost. This modified BC is called BC2. The value of the Lagrange multiplier becomes constant after a while (see Fig. 7(d)), and the reward will eventually reach the same level as that of the MECL case, as shown in Fig. 7(c).

Given the above reasoning, we conclude that the difference in the reward metric between MECL and BC is mainly attributed to the policy learning procedure, not the learned constraint since both MECL and BC achieve the same constraint learning performance as demonstrated in Fig. 7(a). This conclusion is contradicted to the previous paper [3]. And it is important to also directly evaluate the learned constraint, which is less affected by the performance of the constrained RL adopted.

Most papers evaluate the constraint with only one of the two described classes. As mentioned in 3.1, both categories of metrics are utilized in this work. In the first category, IoU (the intersection over union, also known as the Jaccard index) is employed to quantify the correctness of the learned constraints. IoU is widely used in the object detection domain. Recovering the area of the state space that corresponds to the constraint bears similarity to finding the region of the image that contains an object. Therefore, this paper suggests utilizing the IoU as a metric to evaluate the precision of the learned constraint since it encapsulates both the shape of the learned constraint and its location. In the second category, the violation rate of the true constraint by the trained policy is chosen as a metric.